Microbiology (2004), **150**, 1015–1022 DOI 10.1099/mic.0.26828-0

Relations between macroscopic and microscopic adhesion of *Streptococcus mitis* strains to surfaces

Virginia Vadillo-Rodríguez,[1] Henk J. Busscher,[1] Willem Norde,[1,2] Joop de Vries[1] and Henny C. van der Mei[1]

[1]Department of Biomedical Engineering, University of Groningen, Antonius Deusinglaan 1, 9713 AV Groningen, The Netherlands

[2]Laboratory of Physical Chemistry and Colloid Science, Wageningen University, Dreijenplein 6, 6703 HB Wageningen, The Netherlands

Correspondence
Henny C. van der Mei
H.C.van.der.Mei@med.rug.nl

Received 13 October 2003
Revised 1 December 2003
Accepted 19 December 2003

Application of physico-chemical models to describe bacterial adhesion to surfaces has hitherto only been partly successful due to the structural and chemical heterogeneities of bacterial surfaces, which remain largely unaccounted for in macroscopic physico-chemical characterizations of the cell surfaces. In this study, the authors attempted to correlate microscopic adhesion of a collection of nine *Streptococcus mitis* strains to the negatively charged, hydrophilic silicon nitride tip of an atomic force microscope (AFM) with macroscopic adhesion of the strains to a negatively charged, hydrophilic glass in a parallel-plate flow chamber. The repulsive force probed by AFM upon approach of the tip to a bacterial cell surface ranged from 1·7 to 7·7 nN depending on the strain considered and was found to correspond to an activation barrier, governing initial, macroscopic adhesion of the organisms to the glass surface. Moreover, maximum distances at which attractive forces were probed by the AFM upon retraction of the tip (120 to 1186 nm) were related to the area blocked by an adhering bacterium, i.e. the distance kept between adhering bacteria. Bacterial desorption could not be related to adhesive forces as probed by the AFM, possibly due to the distinct nature of the desorption process occurring in the parallel-plate flow chamber and the forced detachment in AFM.

INTRODUCTION

Bacterial adhesion to surfaces is ubiquitous and known to play an important role in a wide variety of environments, as on biomedical implants in the human body (Harkes *et al.*, 1991), on food-processing equipment (Visser & Jeurnink, 1997), on ship hulls (Cooksey & Wigglesworth-Cooksey, 1995), to surfaces in the oral cavity (Marsh & Martin, 1992) and wastewater plants (Characklis, 1973). However, the fundamental mechanisms governing bacterial adhesion are still poorly understood and have not been well defined. Initial bacterial attraction or repulsion to a surface may be described in terms of colloidal interactions. Thus, as bacteria move toward a substratum surface, the initial interaction between a bacterium and the surface is governed by long- and medium-range forces, primarily Lifshitz–Van der Waals and electrostatic forces. In addition, at close approach, other short-range, stereospecific interactions may mediate irreversible adhesion of bacteria to a surface (Rijnaarts *et al.*, 1995). All these interaction forces depend on physico-chemical properties of the substratum and the bacterial surfaces, such as hydrophobicity (Gannon *et al.*, 1991), interfacial tensions (Busscher *et al.*, 1984) and charge (Gannon *et al.*, 1991). These properties are macroscopic in nature and represent an overall expression of the interactions taking place at a microscopic level. Previous studies have attempted to correlate bacterial adhesion with the macroscopic properties of both the substratum and the bacterial cell surfaces. In some cases, bacterial adhesion was related to the surface free energy of the bacteria and/or the substratum, whereas in other cases no relations could be detected (Absolom *et al.*, 1983; Van Pelt *et al.*, 1985). Nearly all bacterial cell surfaces found in nature are negatively charged and they are expected to be repelled by negatively charged substratum surfaces. However, even though experimental studies have shown the importance of electrostatic interactions in bacterial adhesion, discrepancies between experimental observations and theoretical expectations are frequently observed (Ong *et al.*, 1999; Rijnaarts *et al.*, 1995). For instance, adhesion of *Escherichia coli* to sludge flocs did not correlate with the bacterial zeta potential but with the fraction of positive charge present on the bacterial cell surface (Zita & Hermansson, 1997). Similarly, it was shown

Abbreviations: AFM, atomic force microscope (or microscopy); DLVO, Derjaguin, Landau, Verwey, Overbeek; X-DLVO, extended DLVO.

that despite small differences in DLVO (Derjaguin, Landau, Verwey, Overbeek) interaction energies, adhesion rates to glass differed strongly between fibrillated and non-fibrillated *Streptococcus salivarius* strains (Sjollema *et al.*, 1990). Therefore, it can be concluded that the DLVO theory, which accounts for long-range Lifshitz–Van der Waals and electrostatic interactions, has only been marginally successful in describing adhesion of biological particles, such as bacteria, to surfaces. The same conclusion holds for the so-called extended DLVO theory (Van Oss *et al.*, 1986), which also accounts for short-range acid–base interactions between a colloidal particle and a substratum surface.

Until recently, bacterial adhesion has been evaluated mainly by enumeration of the number of bacteria adhering to a surface (An & Friedman, 1997). The parallel-plate flow chamber has turned out to be an effective tool for studying bacterial adhesion to surfaces (McClaine & Ford, 2002). With the aid of phase-contrast microscopy, ultra-long-working-distance objectives and image analysis, bacterial adhesion can be monitored in real time and enumeration is instantaneous under the shear conditions of the actual experiments. The use of flow devices, however, is time-consuming and results provide no quantitative information on the magnitude of the interaction forces between bacteria and a surface.

Atomic force microscopy (AFM) provides new possibilities for probing the structural and physical properties of bacterial cells, as well as information on interaction forces involved in adhesion (Dufrêne, 2000, 2002). Using topographic imaging, cell surface nanostructures (e.g. appendages and flagella) have been visualized, including changes of cell surface morphology during physiological processes. *E. coli* JM109 and K12J169, for instance, have been found to possess different morphologies depending on whether topographic images were taken in liquid or in air. Imaging in air revealed many topographic features that were missing for the cells imaged in liquid. The loss of topographic features in liquid was attributed to the dynamics of cellular filaments, which may collapse onto the wall surface, creating a strain-specific topography of the surface. Furthermore, it was observed that lysozyme treatment led to the loss of surface rigidity and eventually to dramatic changes in bacterial shapes (Bolshakova *et al.*, 2001). Force–distance curves provide complementary information on surface properties, including viscoelasticity and localized surface charge density and hydrophobicity. Interestingly, forces measured between the AFM tip and sulfate-reducing bacteria showed that the adhesion forces at both the cell–substratum periphery and the cell–cell interface were higher than those measured in the centre top of the bacterial cell. This has been suggested to be due to the accumulation of extracellular polymeric substances in interfacial regions (Fang *et al.*, 2000). The role of hydrophobic interactions in bacterial adhesion at a microscopic level has been pointed out by Ong *et al.* (1999), measuring the interaction forces between *E. coli*-coated AFM probes and solids of different surface hydrophobicity. It was shown that both attractive forces and cell adhesion were promoted by the hydrophobicity of the substratum surfaces.

Streptococcus mitis is one of the primary colonizers of surfaces in the oral cavity and it colonizes both dental hard tissues and mucous membranes, most notably the cheeks and the tongue (Marsh & Martin, 1992). By comparison with other oral streptococci, *S. mitis* usually carries sparsely distributed but extremely long fibrils, as demonstrated by electron microscopy (Cowan *et al.*, 1992). It is thought that bacterial surface appendages could exert localized attraction and consequently function to bridge a gap between substratum and the bacterial cell during adhesion (Smit *et al.*, 1986).

The aim of the present study was to relate microscopic adhesion properties of *S. mitis* strains as derived from force–distance curves obtained using AFM to their macroscopic adhesion to surfaces in a parallel-plate flow chamber.

METHODS

Bacterial strains, growth conditions and harvesting. Nine *S. mitis* strains were used in this study, which were all cultured in Todd–Hewitt Broth (Oxoid). For each experiment, the strains were inoculated from blood agar in a batch culture. This culture was used to inoculate a second culture that was grown for 16 h prior to harvesting. Bacteria were harvested by centrifugation (5 min at 10 000 ***g***), washed twice with demineralized water and resuspended in water. To break up bacterial chains, cells were sonicated for 30 s at 30 W (Vibra Cell model 375, Sonics and Materials Inc.). Sonication was done intermittently while cooling in an ice/water bath. These conditions were found not to cause cell lysis in any strain.

Parallel-plate flow chamber and data analysis. The flow chamber (internal dimensions: $76 \times 38 \times 0{\cdot}6$ mm) and image analysis system have been described in detail previously (Busscher & Van der Mei, 1995). Images were taken from the bottom glass plate (55×38 mm) of the parallel-flow chamber. The top plate of the chamber was also made of glass. Glass plates were cleaned by sonicating for 2 min in 2 % RBS35 surfactant solution in water (Omnilabo International), rinsed thoroughly with tap water, dipped in methanol, and again rinsed with demineralized water. The flow chamber was cleaned with Extran (Merck) and thoroughly rinsed with water and demineralized water. Prior to each experiment, all tubes and the flow chamber were filled with 0·1 M KCl solution, taking care to remove all air bubbles from the system. Once the system was filled, a bacterial suspension of 3×10^8 cells ml^{-1} in 0·1 M KCl was allowed to flow through the system at a flow rate of 1·44 ml min^{-1}, corresponding to a Reynolds number of 0·6 and a shear rate at the wall of the flow chamber of 10·6 s^{-1}. Deposition was observed with a CCD-MXRi camera (High technology) mounted on a phase-contrast microscope (Olympus BH-2) equipped with a $\times 40$ ultra-long-working-distance lens (Olympus ULWD-CD Plan 40 PL). The camera was coupled to an image analyser (TEA; Difa). The bacterial suspension was perfused through the system for 4 h with recirculation at room temperature.

The total number of adhering bacteria per unit area $n(t)$ was recorded as a function of time by image sequence analysis during 4 h and the affinity of an organism for the glass surface was expressed as the initial deposition rate j_0, representing the initial increase of $n(t)$ with time (see also Fig. 1). Note that since the initial deposition rate is extracted

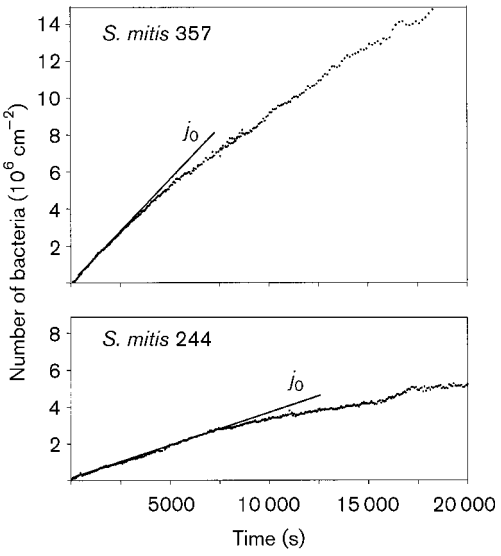

Fig. 1. Number of bacteria deposited as a function of time to a glass surface in 0·1 M KCl as determined in a parallel-flow chamber, for *S. mitis* 357 and *S. mitis* 244.

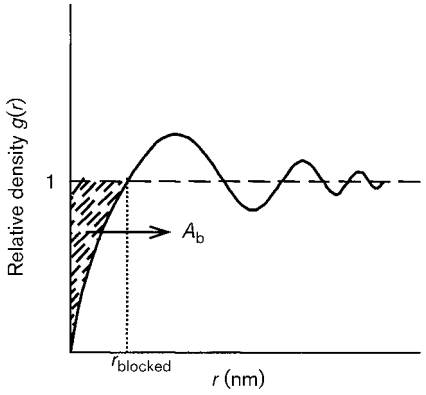

Fig. 2. Relative density of adhering micro-organisms, expressed as a radial pair distribution function $g(r)$ as a function of the distance r between the adhering organisms. The region where $g(r)<1$ is associated with the blocked area A_b.

only from the first, initial adhesion data, it represents the affinity of the organisms for the substratum surface without intervening influences of interactions between adhering bacteria. From the total number of adhering bacteria per unit area as function of time $n(t)$ and the number of particles adhering over the full duration of an experiment n_∞, i.e. saturation adhesion, the so-called characteristic adhesion time τ was calculated using

$$n(t)=n_\infty(1-e^{-t/\tau}) \quad (1)$$

The characteristic adhesion time τ is determined by a combination of deposition, blocking and desorption, according to

$$1/\tau=\beta+j_0A_b \quad (2)$$

in which A_b represents the area on the substratum surface blocked by one adhering bacterium and β is the desorption rate coefficient (Bos *et al.*, 1999). In order to derive the two unknowns A_b and β from equation 2, blocked areas for each particular strain were derived from the radial pair distribution $g(r)$, as can be calculated from the spatial arrangement of the adhering bacteria (Sjollema *et al.*, 1990). Radial pair distribution functions describe the relative density of adhering organisms around a given centre organism as a function of distance between the adhering organisms. Fig. 2 shows an example of a radial distribution function, indicating the region for which $g(r)<1$, i.e. where the density of adhering organisms is less than the mean. Inserting the blocked areas A_b derived from the radial distribution functions, and the characteristic adhesion times τ from the measured kinetics, the desorption rate coefficients β can be directly calculated from equation 2.

All values given in this paper are the mean of three experiments carried out with separately grown micro-organisms.

Atomic force microscopy. Bacterial cells were suspended in water to a concentration of 10^5 ml^{-1}, after which 10 ml of the suspension was filtered through an Isopore polycarbonate membrane (Millipore) with a pore size of 0·8 μm (Dufrêne *et al.*, 1999). The pore size was chosen slightly smaller than the streptococcal dimensions, to immobilize the bacteria by mechanical trapping. After filtration, the filter was carefully fixed with double-sided sticky tape on a sample glass and transferred to the AFM. AFM measurements were made at room temperature under 0·1 M KCl solution, using an optical lever microscope (Nanoscope III, Digital Instruments) with an applied force maintained below 1 nN and a scan rate of ~2 Hz. 'V'-shaped silicon nitride cantilevers from Park Scientific Instruments with a spring constant of 0·06 N m^{-1} and a probe curvature radius of ~50 nm, according to the manufacturer's specifications, were used. Individual force curves with z-displacements of 100–200 nm were collected at z-scan rates ⩽1 Hz. The slope of the retraction force curves in the region where probe and sample are in contact was used to convert the voltage into cantilever deflection. The conversion of deflection data to force data was carried out as has been previously described by others (Dufrêne, 2000).

Topographic images were recorded for at least ten bacterial cells per culture of each *S. mitis* strain. To this end, the tip was positioned over the top of a trapped bacterium, scanning was stopped and ten force measurements were performed at randomly selected locations around the top for each bacterial cell studied. Force–distance curves for both approach and retract interactions were analysed as follows.

Approach. To quantify steric interactions between the AFM tip and cell surface polymers upon approach, a model developed for grafted polymers at relatively high surface coverage was used. The force per unit area between two parallel flat surfaces (F_{st}) with only one coated with polymer has been modelled following the work of Alexander (1977) and De Gennes (1987). To describe the force between a spherical AFM tip and a flat surface, the model was modified by Butt *et al.* (1999) by integrating the force per unit area over the tip surface to produce the interaction force

$$F_{st}=50k_BTaL_0\Gamma^{3/2}\exp(-2\pi h/L_0) \quad (3)$$

where k_B is the Boltzmann constant, T the temperature, a the tip radius, Γ the grafted polymer density per unit area, h the separation distance between the two surfaces and L_0 the equilibrium thickness of the polymer layer. For these calculations the tip radius was assumed to be 250 nm (Drummond & Senden, 1994).

Retraction. Retraction curves of all nine *S. mitis* strains showed various local attractive maxima. These attractive maxima and the distances at which they occurred were quantitatively registered in histograms (see Fig. 3). Based on the relative prevalence of the local

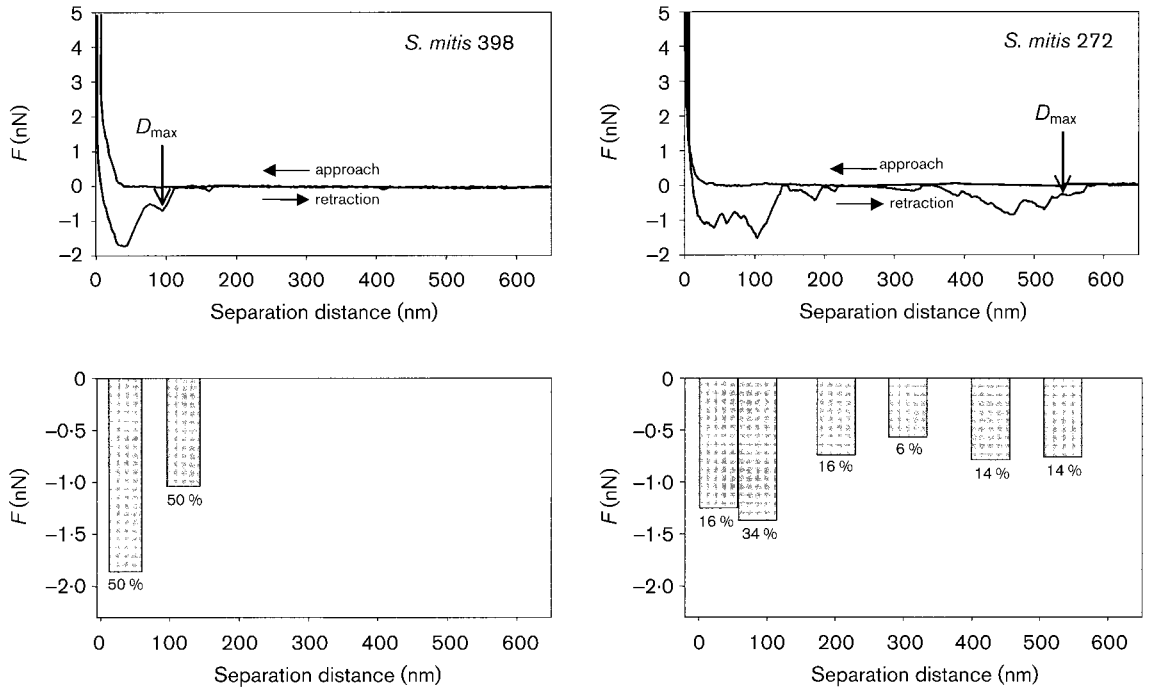

Fig. 3. Retracting force–distance curves and force distribution histograms for *S. mitis* 398 and *S. mitis* 272 in 0·1 M KCl. Local maxima in adhesion force during retraction are marked by arrows for the maximum distance at which they occur. The relative prevalence of each force, as derived from force–distance curves, is indicated in the histograms.

maxima in adhesion forces (expressed in percentages in the histograms), a mean attractive force $F_{adh,\ mean}$ between the AFM tip and the cell surface of each *S. mitis* strain was calculated. Forces with prevalence less than 2 % were neglected in this averaging process.

Theory. The results obtained in this study were explained on the basis of a combination of the extended DLVO (X-DLVO) theory and the steric model accounting for repulsion between bacterial polysaccharide molecules and the AFM tip, described above. The X-DLVO model accounts for Van der Waals, electrical double layer and acid–base interactions. The expressions quantifying these interactions as a function of separation distance can be found elsewhere (Van Oss, 1994) for different system geometries. The radius of the AFM tip was assumed to be small relative to the curvature of the bacterium, and therefore the tip was approximated as a sphere and the bacterium as a flat surface (Johnson *et al.*, 1995). A Hamaker constant of 10^{-20} J was chosen, consistent with earlier work on bacterial adhesion (Martin *et al.*, 1996). Bacterial zeta potentials were recalculated from the surface fixed charge density previously obtained in a recent publication (Vadillo-Rodriguez *et al.*, 2002) for all nine *S. mitis* strains by soft particle analysis according to Ohshima (Ohshima & Kondo, 1991), yielding a mean surface potential of −1·6 mV. For silicon nitride tips, the zeta potential was estimated from electrophoretic mobility measurements on silicon nitride particles as a function of the pH (Harkes *et al.*, 1991) and taken as −2·0 mV in our calculations. Acid–base interactions were estimated based on electron-acceptor γ^+ and electron-donor γ^- parameters (Van Oss, 1994). These parameters were calculated for glass and bacteria by means of the Young–Dupré equation after measuring contact angles with four different liquids (Cowan *et al.*, 1992). The resulting values amount to $\gamma^+ = 1{\cdot}5$ mJ m^{-2}, $\gamma^- = 56{\cdot}3$ mJ m^{-2} for glass and to mean values $\gamma^+ = 2{\cdot}1$ mJ m^{-2} and $\gamma^- = 5{\cdot}7$ mJ m^{-2} for the *S. mitis* strains.

Fig. 4 shows the result of this modelling, displaying the interaction forces as divided by the effective radius of the tip.

RESULTS

Fig. 1 presents examples of the deposition rates for *S. mitis* 357 and 244 to a glass surface in 0·1 M KCl. The deposition

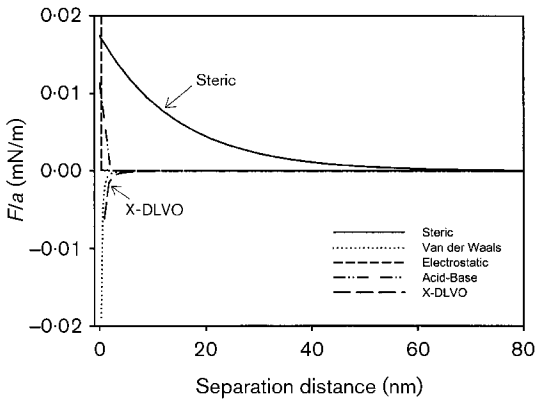

Fig. 4. The interaction force (divided by the radius of the AFM tip) between an AFM tip and a bacterial cell surface as a function of separation distance, based on X-DLVO theory and steric repulsions, as arising from mean input values of the total collection of *S. mitis* isolates and a silicon nitride tip in 0·1 M KCl.

Table 1. Initial deposition rates j_0, blocked areas A_b and desorption rate coefficients β of *S. mitis* strains adhering to a glass surface

Experiments were done with cells suspended in 0·1 M KCl in a parallel-plate flow chamber. Initial deposition rates j_0 were calculated from the initial linear increase of the number of adhering bacteria with time, and blocked areas A_b from the radial pair distribution functions. The results are means ± SD of three separate experiments with separately cultured organisms.

S. mitis strain	j_0 (cm^{-2} s^{-1})	A_b (μm^2)	β (10^{-5} s^{-1})
ATCC 9811	542 ± 134	1·1 ± 0·2	10·9 ± 2·7
ATCC 33399	439 ± 49	1·5 ± 1·2	2·5 ± 0·3
244	305 ± 29	1·1 ± 0·2	4·1 ± 1·2
272	443 ± 117	1·4 ± 0·4	1·8 ± 0·7
357	970 ± 159	1·9 ± 0·4	1·8 ± 0·4
398	827 ± 184	1·8 ± 0·2	4·8 ± 1·7
BMS	601 ± 111	1·3 ± 0·3	5·8 ± 2·2
BA	492 ± 85	0·7 ± 0·2	6·5 ± 1·8
T9	388 ± 76	1·0 ± 0·1	5·0 ± 0·2

behaviour of all nine *S. mitis* strains followed an exponential rise with time to a maximum value, of which the initial linear part allowed calculation of the initial deposition rate j_0. Blocked areas were determined from radial pair distribution functions and are summarized in Table 1, together with the initial deposition rates and the desorption rate coefficients β. As can be seen, *S. mitis* strains present varying adhesive abilities. For instance, the initial deposition rate j_0 of *S. mitis* 357 is three times higher than that of *S. mitis* 244 and blocked areas A_b range from 0·7 μm^2 for *S. mitis* BA to 1·9 μm^2 for *S. mitis* 357. Desorption rate coefficients are generally small (on the average 10^{-5} s^{-1}) and are somewhat higher for *S. mitis* ATCC 9811 than for the other bacterial strains.

Fig. 3 shows two examples of the interaction forces measured between *S. mitis* 398 and *S. mitis* 272 and a silicon nitride AFM tip immersed in 0·1 M KCl as a function of the separation distance between the tip and the bacterium. Under our experimental conditions, all nine *S. mitis* strains present a repulsive force upon approach and multiple local maxima in attractive adhesion forces upon retraction. The repulsive forces upon approach indicate an equilibrium length L_0 of the surface polymers between 50 nm and 314 nm, depending on the strain considered (see Table 2). The polymer density Γ, however, ranges from 3×10^{-3} nm^{-2} to 21×10^{-3} nm^{-2} (see also Table 2), in line with the sparse distribution of fibrils carried by *S. mitis* surfaces, as observed by electron microcopy (Cowan *et al.*, 1992).

Upon retraction, the number of multiple local maxima in adhesion forces ranged from two at small separation distances for *S. mitis* 398, to eleven for *S. mitis* T9 at separation distances up to 1186 nm. The separation distances at which these adhesion forces occur, their magnitude and relative prevalence as averaged per strain are summarized in so-called distribution force histograms (see Fig. 3, showing the distribution force histogram for *S. mitis* 398 and 272). The maximal distance D_{max} at which local adhesion forces occur together with the mean adhesion force $F_{adh,\ mean}$ (arising from a bacterial cell surface as calculated from the relative prevalence of all local adhesion forces) and the number N of local maxima in adhesion forces are presented in Table 2. The mean adhesion force $F_{adh,\ mean}$ ranges from −0·5 nN to −2·2 nN, depending on the strain considered. The large standard deviations associated with the values may be attributed the heterogeneous nature of the *S. mitis* cell surfaces.

Relations found between microscopic adhesion properties of *S. mitis* strains as derived from force–distance curves analysis and macroscopic adhesion in the parallel-plate

Table 2. Summary of quantitative data derived from force–distance curves in 0·1 M KCl of nine *S. mitis* strains

The data tabulated are: from approach curves, equilibrium length L_0 of the bacterial surface polymers, bacterial polymer density Γ and force at zero separation distance F_{st} ($h=0$); and from retraction curves, maximum distances D_{max} at which local maxima in adhesion force occur, together with the number of local maxima (N) and the mean adhesion force $F_{adh,\ mean}$ calculated.

S. mitis strain	Approach			Retraction		N
	L_0 (nm)	Γ (10^{15} m^{-2})	F_{st} ($h=0$) (nN)	D_{max} (nm)	$F_{adh,\ mean}$ (nN)	
ATCC 9811	314 ± 37	3 ± 1	2·1 ± 0·8	167 ± 33	−0·5 ± 0·3	2
ATCC 33399	57 ± 12	11 ± 2	3·5 ± 0·7	170 ± 30	−1·4 ± 0·8	3
244	82 ± 18	8 ± 2	2·8 ± 0·7	426 ± 29	−1·8 ± 1·0	4
272	82 ± 37	9 ± 3	3·6 ± 1·4	534 ± 29	−1·0 ± 0·4	6
357	63 ± 12	5 ± 1	1·1 ± 0·2	196 ± 43	−0·7 ± 0·2	3
398	50 ± 6	21 ± 3	7·7 ± 1·0	120 ± 35	−1·5 ± 0·7	2
BMS	63 ± 18	6 ± 3	1·6 ± 0·8	867 ± 40	−1·1 ± 0·4	9
BA	50 ± 6	10 ± 2	2·7 ± 0·6	588 ± 23	−1·4 ± 0·3	5
T9	70 ± 18	12 ± 5	4·8 ± 2·0	1186 ± 38	−2·2 ± 0·9	11

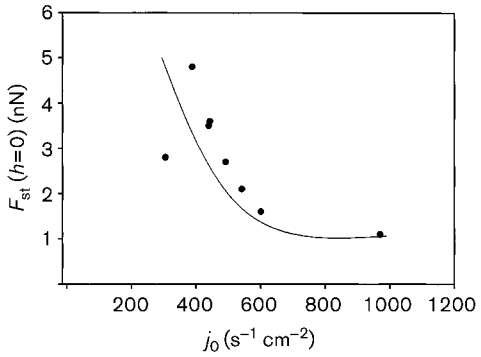

Fig. 5. Force at zero separation distance F_{st} ($h=0$) between the AFM tip and the bacterial cell surface measured upon approach, as a function of the initial deposition rates j_0 of eight *S. mitis* strains to glass, as determined in a parallel-plate flow chamber in 0·1 M KCl.

flow chamber are depicted in Figs 5–7. Fig. 5 shows that the initial deposition rates j_0 decrease as the force needed to achieve contact between the AFM tip and bacterial surface, i.e. F_{st} at zero separation distance, increases, indicating that the bacteria have to overcome a barrier before they can adhere. Note that *S. mitis* 398 constituted an exception to this behaviour for reasons unknown and the strain has been omitted from this analysis. The radius of the area blocked $r_{blocked}$ by an adhering organism decreases in an almost linear fashion with the maximum distance D_{max} over which the adhesion forces detected by the AFM tip upon retraction are operative. Note, in addition, that the order of magnitude of the radii of these blocked areas and the distance over which the adhesion forces act are roughly similar (see Fig. 6), while here *S. mitis* ATCC 9811 constituted an exception. In Fig. 7, it can be seen that, unexpectedly, no relation could be found between the desorption rate coefficients β and the adhesion forces $F_{adh,\ mean}$.

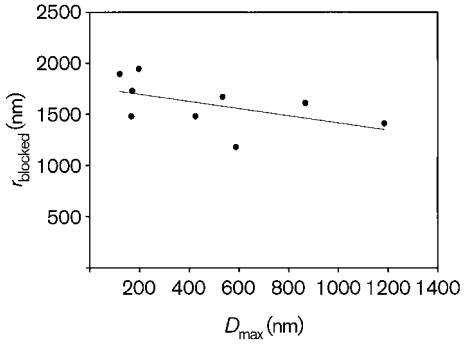

Fig. 6. Radius $r_{blocked}$ of the blocked areas A_b of nine *S. mitis* strains adhering on glass in 0·1 M KCl, as a function of the maximum distance D_{max} at which a local maximum in adhesion force is probed by the AFM tip upon retraction.

DISCUSSION

Physico-chemical models to explain bacterial adhesion to solid substrata have only been partly successful for a limited number of strains, while usually a small number of strains have been involved in the verification of a model. The poor performance, so far, of physico-chemical models for microbial adhesion to surfaces is due in part to the macroscopic approach of the system, which is usually heterogeneous on a microscopic level. Lack of equipment to measure physico-chemical properties of microbial cell surfaces with a microscopic resolution has for a long time impeded progress in the field. With the introduction of the AFM, new possibilities for microscopic characterization of bacterial cell surfaces have become available. In this paper, we relate microscopic characterization of a large number of *S. mitis* strains, as probed by their interaction with the silicon nitride tip of the AFM, to their macroscopic adhesion to glass. High correlations between the two sets of data were expected, since both glass and the silicon nitride tip are hydrophilic and negatively charged. At this stage it is important to note that the relations presented in Figs 5–7 are obtained from a large collection of *S. mitis* strains. Therefore the relations depicted are expected to have a high degree of general validity, although not all strains behave fully according to the general trends we derive from our results.

The approach curves in the AFM measurements were used to assess steric interactions in adhesion of the organisms. The interaction forces given in Fig. 4 demonstrate the relative importance of Lifshitz–Van der Waals, electrostatic, acid–base and steric terms for our collection of strains. X-DLVO interactions decay over a very short distance ($\sim$10 nm) and are therefore less influential on bacterial deposition to a substratum surface than steric forces that extend over much longer distances. Even though the X-DLVO does not show any energy barrier for adhesion, force–distance curves for all nine *S. mitis* strains always presented a repulsive force upon approach. Based on the theoretical predictions and on the distance observed at

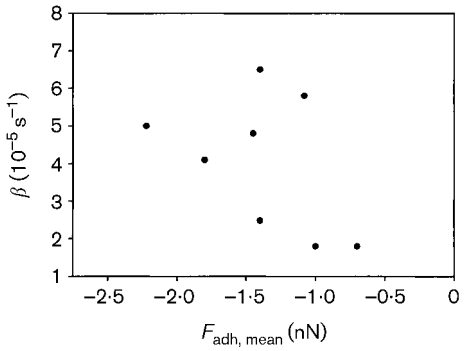

Fig. 7. Desorption rate coefficients β of *S. mitis* strains in 0·1 M KCl as a function of the mean adhesion force $F_{adh,\ mean}$ between the AFM tip and the cell surface upon retraction.

which this repulsive force becomes effective, we conclude that the force–distance curves for approach could only be described in terms of steric repulsion.

The steric interactions as obtained from AFM play an important role in relating microscopic cell surface properties and macroscopic adhesion in the parallel-plate flow chamber. According to X-DLVO theory and based on the analogy between the surface properties of the tip and the glass surface, macroscopic adhesion of *S. mitis* to the glass substratum in the parallel-plate flow chamber occurs under barrierless conditions (see Fig. 4). However, the AFM tip detected a steric energy barrier that must be overcome in order to achieve close contact with the bacterial surface. This energy barrier could be interpreted as an activation energy for the organisms to successfully deposit, as by the relation shown in Fig. 5: the initial deposition rate increases as the force required to overcome the energy barrier by the AFM tip decreases. These forces range between 1·1 and 7·7 nN for the nine *S. mitis* isolates employed in this study, and integrating equation 3 over the entire interaction range yields activation energies of $\sim$2700 kT and 15 000 kT, respectively. These activation energies are prohibitively high for spontaneous adhesion to occur for the entire collection of strains studied. Therefore, even though steric repulsion forces can be used to predict adhesion according to Fig. 5, they are not fully responsible for adhesion at the separation distances at which they become operative.

The steric model is not only useful in explaining aspects of bacterial adhesion to macroscopic surfaces, but also in better understanding the cell surface itself. L_0 defines the equilibrium length of the bacterial surface polymers and under our specific ionic strength conditions amounts to several tens of nanometers, except for *S. mitis* ATCC 9811. Other studies, also on fibrillated strains, reported equilibrium lengths L_0 in the order of several hundreds of nanometers (Camesano & Logan, 2000). The present study was done, however, in a relatively high ionic strength solution, which may condense the electrically charged polymers on the cell surface and yield a relatively thin layer. Macroscopic as well as microscopic measurements at various ionic strengths have provided evidence of a collapse of the fibrillated material at high ionic strength (Van der Mei *et al.*, 1994, 2000).

The initial stages of macroscopic adhesion are governed mainly by interactions between the bacterial cell surfaces and the substratum surface, but in the more advanced stages, adhesion is in essence an interplay between interactions occurring between the substratum surface, a depositing bacterium and an already adhering one. It is interesting that this mechanism is confirmed by the combination of microscopic and macroscopic data shown in Fig. 6. As the distance over which the bacterium exerts adhesive forces extends, for instance through the extension of fibrils of different lengths (Van der Mei *et al.*, 2000), bacteria are brought closer together and the distance between adhering bacteria is reduced (Smit *et al.*, 1986), yielding smaller blocked areas.

Desorption rate coefficients β are generally small for all *S. mitis* strains, on average in the order of $\sim 10^{-5}\ s^{-1}$. The adhesion force measured by the AFM tip upon retraction was expected to be indicative of the desorption of bacteria in the parallel-plate flow chamber. Fig. 7 shows, however, that contrary to our expectation, no clear relation was found. Possibly, this has to do with the nature of the desorption process. Desorption in the parallel-plate flow chamber takes place as a spontaneous process under the prevailing shear conditions, while in AFM the contact between bacterium and surface substratum is forced to break by application of an external force.

Summarizing, this study demonstrates that the repulsive force probed by AFM upon approach of the tip to a bacterial cell surface corresponds to a steric activation energy barrier, governing the rate of initial, macroscopic adhesion of the organisms to a glass surface. Moreover, the maximum distance at which attractive forces are probed by AFM upon retraction of the tip is related to the area blocked by an adhering bacterium (i.e. the distance kept between adhering bacteria), but bacterial desorption could not be related to adhesive forces as probed by the AFM.

REFERENCES

Absolom, D. R., Lamberti, F. V., Policova, Z., Zing, W., Van Oss, C. J. & Neumann, A. W. (1983). Surface thermodynamics of bacterial adhesion. *Appl Environ Microbiol* **46**, 90–97.

Alexander, S. (1977). Adsorption of chain molecules with a polar head. A scaling description. *J Phys II* **38**, 983–987.

An, Y. H. & Friedman, R. J. (1997). Laboratory methods for studies of bacterial adhesion. *J Microbiol Methods* **30**, 141–152.

Bolshakova, A. V., Kiselyovaa, O. I., Filonova, A. S., Frolova, O. Y., Lyubchenkoc, Y. L. & Yaminskya, I. V. (2001). Comparative studies of bacteria with an atomic force microscope operating in different modes. *Ultramicroscopy* **86**, 121–128.

Bos, R., Van der Mei, H. C. & Busscher, H. J. (1999). Physico-chemistry of initial microbial adhesive interactions – its mechanisms and methods for study. *FEMS Microbiol Rev* **23**, 179–230.

Busscher, H. J. & Van der Mei, H. C. (1995). Use of flow chamber devices and image analysis methods to study microbial adhesion. *Methods Enzymol* **253**, 455–477.

Busscher, H. J., Weerkamp, A. H., Van der Mei, H. C., Van Pelt, A. W. J., De Jong, H. P. & Arends, J. (1984). Measurements of the surface free energy of bacterial cell surfaces and its relevance for adhesion. *Appl Environ Microbiol* **48**, 980–983.

Butt, H.-J., Kappl, M., Mueller, H. & Raiteri, R. (1999). Steric forces measured with the atomic force microscope at various temperatures. *Langmuir* **15**, 2559–2565.

Camesano, T. A. & Logan, B. E. (2000). Probing bacterial electrosteric interactions using atomic force microscopy. *Environ Sci Technol* **34**, 3354–3362.

Characklis, W. G. (1973). Attached microbial growths. I. Attachment and growth. *Water Res* **7**, 1113–1127.

Cooksey, K. E. & Wigglesworth-Cooksey, B. (1995). Adhesion of bacteria and diatoms to surfaces in the sea: a review. *Aquat Microb Ecol* **9**, 87–96.

Cowan, M. M., Van der Mei, H. C., Rouxhet, P. G. & Busscher, H. J. (1992). Physico-chemical and structural properties of the surfaces of *Peptostreptococcus micros* and *Streptococcus mitis* as compared to those of mutans streptococci, *Streptococcus sanguis* and *Streptococcus salivarius*. *J Gen Microbiol* **138**, 2707–2714.

De Gennes, P. G. (1987). Polymers at an interface; a simplified view. *Adv Colloid Interface Sci* **27**, 189–209.

Drummond, C. J. & Senden, T. J. (1994). Examination of the geometry of long-range tip–sample interaction in atomic force microscopy. *Colloids Surf A: Physicochem Eng Aspects* **87**, 217–234.

Dufrêne, Y. F. (2000). Direct characterization of the physicochemical properties of fungal spores using functionalized AFM probes. *Biophys J* **78**, 3286–3291.

Dufrêne, Y. F. (2002). Atomic force microscopy, a powerful tool in microbiology. *J Bacteriol* **184**, 5205–5213.

Dufrêne, Y. F., Boonaert, C. J. P., Gerin, P. A., Asther, M. & Rouxhet, P. G. (1999). Direct probing of the surface ultrastructure and molecular interactions of dormant and germinating spores of *Phanerochaete chrysosporium*. *J Bacteriol* **181**, 5350–5354.

Fang, H. H. P., Chan, K.-Y. & Xu, L.-C. (2000). Quantification of bacterial adhesion forces using atomic force microscopy (AFM). *J Microbiol Methods* **40**, 89–97.

Gannon, J. T., Manilal, V. B. & Alexander, M. (1991). Relationships between cell surface properties and transport of bacteria through soil. *Appl Environ Microbiol* **57**, 190–193.

Harkes, G., Feijen, J. & Dankert, J. (1991). Adhesion of *Escherichia coli* on to a series of poly(methacrylates) differing in charge and hydrophobicity. *Biomaterials* **12**, 853–860.

Johnson, S. B., Drummond, C. J., Scales, P. J. & Nishimura, S. (1995). Comparison of techniques for measuring the electrical double layer properties of surfaces in aqueous solution: hexadecyltrimethylammonium bromide self-assembly. *Langmuir* **11**, 2367–2375.

Marsh, P. & Martin, M. (1992). *Oral Microbiology*, 3rd edn. London: Chapman & Hall.

Martin, M. J., Logan, B. E., Johnson, W. P., Jewett, D. G. & Arnold, R. G. (1996). Scaling bacterial filtration rates in different sized porous media. *J Environ Eng* **122**, 407–415.

McClaine, J. W. & Ford, R. M. (2002). Characterizing the adhesion of motile and nonmotile *Escherichia coli* to a glass surface using a parallel-plate flow chamber. *Biotechnol Bioeng* **78**, 179–189.

Ohshima, H. & Kondo, T. (1991). On the electrophoretic mobility of biological cells. *Biophys Chem* **39**, 191–198.

Ong, Y. L., Razatos, A., Gerogiou, G. & Sharma, M. M. (1999). Adhesion between *E. coli* bacteria and biomaterial surfaces. *Langmuir* **15**, 2719–2725.

Rijnaarts, H. H. M., Norde, W., Bouwer, E. J., Lyklema, J. & Zehnder, A. J. B. (1995). Reversibility and mechanism of bacterial adhesion. *Colloids Surf B* **4**, 5–22.

Rijnaarts, H. H. M., Norde, W., Lyklema, J. & Zehnder, A. J. B. (1999). DLVO and steric contributions to bacterial deposition in media of different ionic strengths. *Colloids Surf B* **14**, 179–185.

Sjollema, J., Van der Mei, H. C., Uyen, H. M. W. & Busscher, H. J. (1990). The influence of collector and bacterial cell surface properties on the deposition of oral streptococci in a parallel plate flow cell. *Adh Sci Technol* **4**, 765–779.

Smit, G., Kijne, J. W. & Lugtenbert, B. J. J. (1986). Correlation between extracellular fibrils and attachment of *Rhizobium leguminosarum* to pea root hair tips. *J Bacteriol* **169**, 4294–4301.

Vadillo-Rodriguez, V., Busscher, H. J., Norde, W. & Van der Mei, H. C. (2002). Softness of the bacterial cell wall of *Streptococcus mitis* as probed my microelectrophoresis. *Electrophoresis* **23**, 2007–2011.

Van der Mei, H. C., Meinders, J. M. & Busscher, H. J. (1994). The influence of ionic strength and pH on diffusion of micro-organisms with different structural surface features. *Microbiology* **140**, 3413–3419.

Van der Mei, H. C., Busscher, H. J., Bos, R., De Vries, J., Boonaert, C. J. P. & Dufrêne, Y. F. (2000). Direct probing by atomic force microscopy of the cell surface softness of a fibrillated and nonfibrillated oral streptoccal strain. *Biophys J* **78**, 2668–2674.

Van Oss, C. J. (1994). *Interfacial Forces in Aqueous Media*. New York: Marcel Dekker.

Van Oss, C. J., Good, R. J. & Chaudhury, M. (1986). The role of Van der Waals forces and hydrogen bonds in hydrophobic interactions between biopolymers and low energy surfaces. *J Colloid Interface Sci* **111**, 378–390.

Van Pelt, A. W., Weerkamp, A. H., Uyen, M. H., Busscher, H. J., De Jong, H. P. & Arends, J. (1985). Adhesion of *Streptococcus sanguis* CH3 to polymers with different surface free energies. *Appl Environ Microbiol* **49**, 1270–1275.

Visser, J. & Jeurnink, T. J. M. (1997). Fouling of heat exchangers in the dairy industry. *Exp Therm Fluid Sci* **14**, 407–424.

Zita, A. & Hermansson, M. (1997). Effects of bacterial cell surface structures and hydrophobicity on attachment to activated sludge flocs. *Appl Environ Microbiol* **63**, 1168–1170.